2017

Design of Quad Tiltrotor Attitude Control Experiment for Control System Education

Zhuogang Peng
Lehigh University

Design of Quad Tiltrotor Attitude Control Experiment for Control System Education

by

Zhuogang Peng

Presented to the Graduate and Research Committee of Lehigh University in Candidacy for the Degree of Master of Science

in

Mechanical Engineering

Lehigh University

Department of Mechanical Engineering and Mechanics

Bethlehem, PA 18015

July 24, 2017

Certificate of Approval

This thesis is accepted and approved in partial fulfillment of the requirements for the Master of Science in Electrical Engineering.

July 24, 2017

Date

Professor Eugenio Schuster

Thesis Advisor

Professor Gary Harlow

Chairperson of Department

Acknowledgements

First, I would like to express my gratitude to my advisor, Professor Eugenio Schuster, for his guidance and support on this project. I am deeply grateful for his encouragement and assistance.

I would also like to thank my parents, Li and Mingxia, as well as the rest of my family for their continued support of my education.

Contents

List of Figures

Abstract

The quad tiltrotor is a vertical take-off and landing UAV (Unmanned Aerial Vehicle). It has four propellers, each of which is mounted on four separate gimbals. This thesis presents an experimental design for the quad tiltrotor's attitude controller.

First, we detailed the mechatronic system of the quad tiltrotor and assembled the prototype. Then we derived the dynamic model using the Lagrangian method. Next, we designed a PID controller for our prototype using the feedback linearization method. Then we ran simulations. The results showed that our controller performed well when it came to tracking and stability. We also implemented the controller to the Pixhawk flight control board of our quad tiltrotor. Finally, we designed an experiment to test our attitude controller. The results analysis, which was performed with a MATLAB GUI that we developed, demonstrated that our design is practicable and flexible.

Chapter 1

Introduction

1.1 Background to Quadrotor

The quadrotor UAV (Unmanned Aerial Vehicle) is a vertical take-off and landing aircraft with six degrees of freedom. The quadrotor can perform tasks that fixed-wing aerial vehicles cannot: it can hover, fly with low speed, take off vertically, and land and fly indoors. In general, the quadrotor has the advantages of simple structure and control, the low requirement of manufacturing accuracy, reliable stability, and weak gyroscopic effects [1], [2].

A common quadrotor model is equipped with two pairs of identical propellers. One pair or propellers spins clockwise; the other pair spins counterclockwise [3]. The force produced by the propellers is proportional to the square of the angular velocity of the motors [4]. By changing the speed of each rotor, the quadrotor can generate a desired total thrust, torque, or turning force. Since the quadrotor is structurally symmetrical, there is no practical difference between the left and right. As such, the vehicle has the logistical flexibility to take off in any direction.

The quadrotor has a highly coupled dynamic characteristic which means a change

in one rotor speed will result in variations in three freedom degrees at least. For example, reducing the rate of the right rotor will cause the quadrotor to roll right because of the imbalance between the left and right lifts. Meanwhile, the quadrotor will make a right yaw for the torque imbalance of two groups of rotors. Furthermore, the rolling will cause the quadrotor to shift to the right because the direction of the force of the quadrotor is now bottom-left. The yaw movement causes translation, which changes the quadrotor's direction of movement [5].

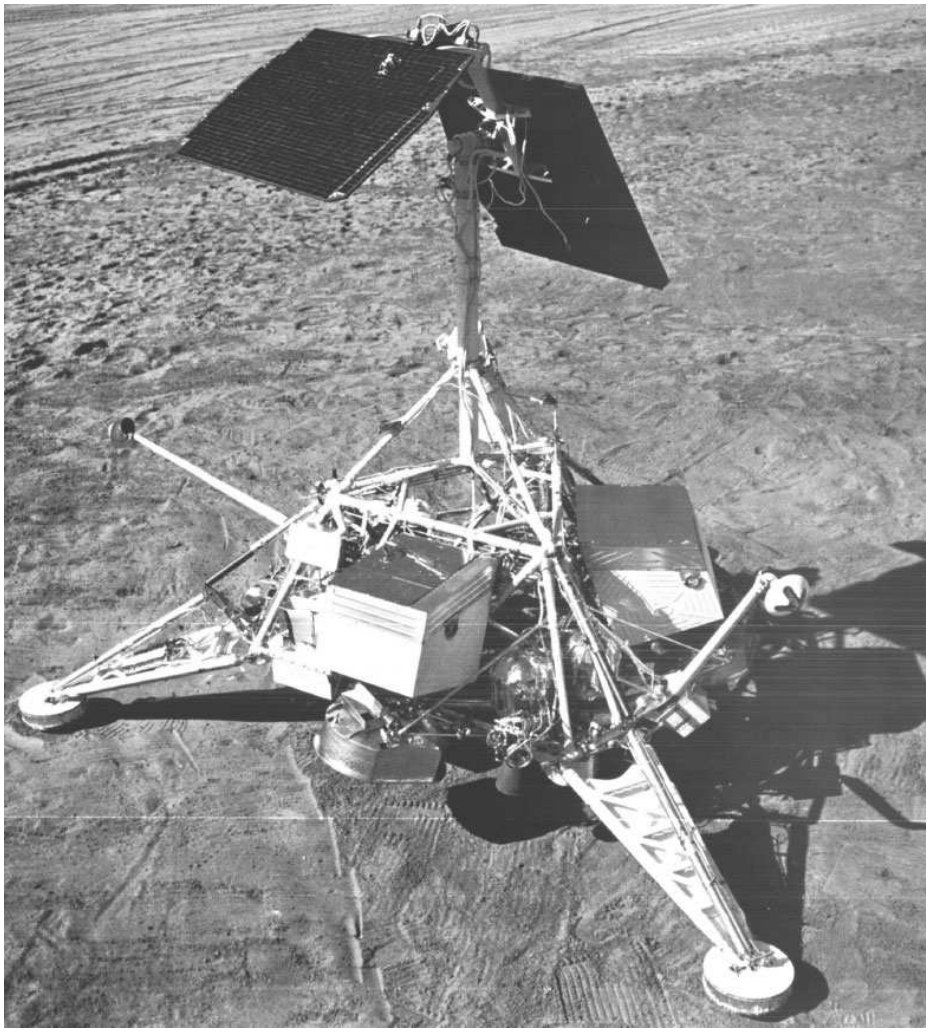

Figure 1.1: NASA's lunar lander, "Surveyor."

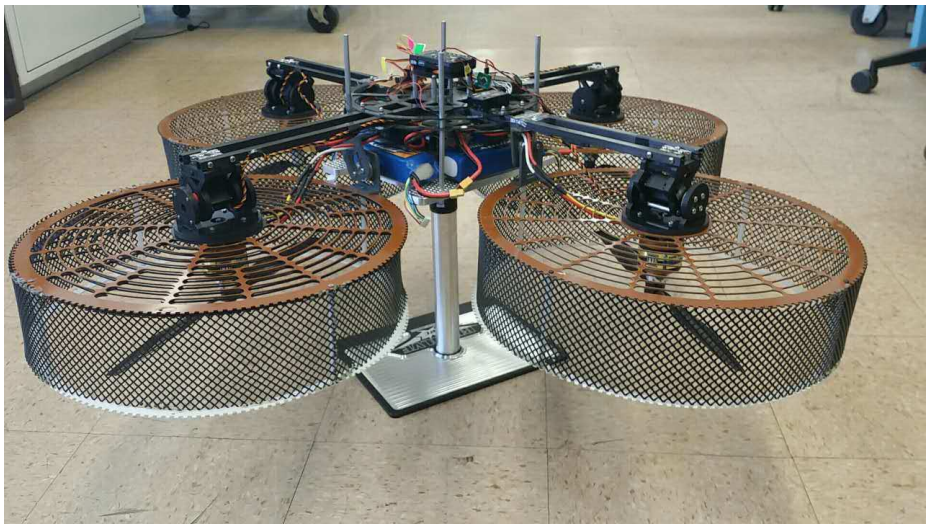

Figure 1.2: Our quad tiltrotor prototype.

1.2 Our Quad Tiltrotor Prototype

This thesis focuses on the "quad tiltrotor," a quadrotor concept in which each propeller has one more gimbal than is found on standard quadrotor propellers. A wider variety of control strategies is available for the quad tiltrotor because the vectored thrust of each propeller makes it possible to control the vehicle's altitude and position separately.

The structure of the quad tiltrotor that is discussed in this thesis was inspired by NASA's sixth lunar lander, "Surveyor-6," which was a hopping spacecraft (Figure 1.1) [6]. Figure 1.2 shows our quad tiltrotor prototype. The actuators of our quad tiltrotor are four rotors mounted on four single-axis gimbals whose angle is controlled by a servo. Each rotor produces both a thrust and torque about its center of rotation, as well as a drag force opposite to the vehicle's direction of flight. If all propellers are spinning at the same angular velocity but with different directions, with two rotating clockwise and the other two rotating counterclockwise, the yaw angle can still be changed.

1.3 Mechatronics

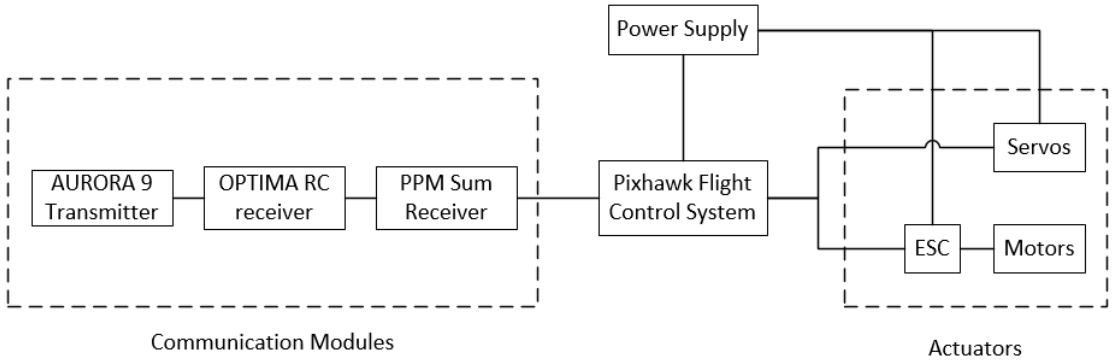

Figure 1.3: Quad tiltrotor mechatronic system

As Figure 1.3 shows, our quad tiltrotor's mechatronic system consists of communication modules, a flight controller board, actuators and power supplies. The communications between an operator and our quad tiltrotor were conveyed by a remote transmitter and an RC receiver. The remote transmitter produced control signals and the RC receiver received the signals. We used the PX4 autopilot (Pixhawk) as our flight control board. By making a real-time comparison of the current attitude (that was detected by IMU (Inertial Measurement Unit) sensors) with the goal attitude (determined by input signals), our Pixhawk can calculate the desired outputs to control the actuators. The actuators include four motors and four servos. Our servos are controlled by Pixhawk outputs directly while our motors need ESC (Electronic Speed Control) to transform the PWM output signals to three-phase electric power and drive them. To power the actuators and the Pixhawk board, we connect four Lipo batteries in parallel using power distribution boards.

1.4 Control Method

The quad tiltrotor has six state variables (three positions and three attitudes) and eight control inputs (rotors speed and servos angle), which make it an over-actuated system because the number of inputs exceeds the number of freedom degrees by two. Designing the flight control system is difficult because the controller performance is affected by the accuracy of the model and the accuracy of the sensors [7], [8], [9].

In recent years, many researchers have published articles on the quad tiltrotor control problem. The normal movement of a quad tiltrotor includes attitude stabilization and movement (posture and position) from one point to another. Many quad tiltrotor control research papers have focused on the design and verification of the attitude controller [10], [11], [12]. Most of the controllers have good simulation results with the use of nonlinear control laws. However, the actual control performance is often unsatisfactory because of the high dependence on model accuracy [13], [14]. Therefore, there is an urgent need for quad tiltrotor control system researchers to develop a controller which not only controls the aircraft attitude accurately but also offers strong anti-interference and environmental adaptability.

In this work, we used feedback linearization to transform our nonlinear system into an equivalent linear system. In this way, we were able to develop a simple PID controller to track the attitude references.

1.5 Control System Experiment for Education

Laboratory projects are essential for educating engineering majors about control systems. Developing and testing control algorithms helps students consolidate theoretical knowledge and learn how to put that theory into practice [15], [16]. The quad tiltrotor's unstable dynamics and tight integration of control electronics make it a

particularly attractive object for experimentation. While studying the quad tiltrotor, students increase their proficiency in the design of control systems and the implementation of hardware systems [17].

In this work, we designed and tested an attitude controller for our quad tiltrotor, which was fixed on a test stand. In the future, students can change the PID parameters of our controller and perform experiments to test the controller's performance. After the experiment, students can analyze the results by using the MATLAB GUI that we designed.

1.6 Thesis Organization

This thesis is organized in the following way: Chapter 2 describes the quad tiltrotor's mechatronic system. Chapter 3 details the development of the quad tiltrotor's dynamic models. Chapter 4 discusses the model-based control strategy and shows the results of simulations ran in Matlab. Chapter 5 explores the possible implementations of the controller. Chapter 6 details the process of our experiments and develops a MATLAB GUI for result analysis. Chapter 7 concludes the thesis.

Chapter 2

Mechatronic System

2.1 Communication Modules

Figure 2.1: The RC receiver and the remote transmitter.

We used a HITEC Aurora 9 transmitter [18] to control the movement of our quad tiltrotor during the experiments. The Aurora 9 has a fully assignable control switch, knob, stick and digital trims. In this work, we controlled throttle, pitch, roll and yaw. Each of these control signals was mapped to transmitter sticks and to the Optima 9 [19], which is a nine-channel 2.4 GHz receiver mounted on our quad

tiltrotor. The signals received by the Optima 9 are PWM (Pulse Width Modulation), but the Pixhawk can only identify PPM (Pulse Position Modulation) signals. So, we used a jDrones V2.1 PPM-Sum encoder [20] to transform the PWM signals into PPM signals.

2.2 Flight Control Board

Figure 2.2: The Pixhawk connector pins.

Pixhawk is an open source autopilot system that comes with built-in IMU sensors including gyroscopes, accelerometers and pressure sensors [21]. The gyroscope, which has excellent dynamic performance and resistance to external interference, can measure the rate of attitude angles. But the integration of errors will accumulate over time due to the gyroscope drift. That is the reason why we need magnetometers and accelerometers. The accelerometer has good low-frequency characteristics and can measure acceleration accurately in static conditions. The magnetometer can measure the Earth's magnetic field. The changes over time in the measurements of the accelerometer and the magnetometer are relatively small. However, they are sensitive to external disturbances and can only get a 2-dimensional angular relationship [22].

In our experiments, we adopted the algorithms found in [23] to fuse three kinds of data, which enabled us to obtain credible attitude angles.

As Figure 2.2 [24] shows, we connected the main PWM OUT pins 1-4 to the ESCs (Electronic Speed Controller), pins 5-8 to the servos and the PPM-SUM IN pins to the PPM encoder. Once we combined the control signals from the communication modules and the attitude data from the IMU sensors, the Pixhawk could calculate the required PWM signals based on the developed control law and output them to the servos and the ESCs.

2.3 Actuators

Our ten-kilogram quad tiltrotor prototype is outfitted with four AXI 4120/18 GOLD LINE brushless motors [25] and four 15"×9.5" propellers, each of which has a maximum thrust of 40 Newtons. The thrust-to-weight ratio of our quad tiltrotor is 1.6. The general ratio requirement for UAVs is 2 [26], [27], but because we fixed the quad tiltrotor in a revolve test stand during our experiments, we don't need such a high thrust-to-weight ratio.

The angles of our HS-5685MH servos [28] range from -30 degrees to 30 degrees and the maximum torque is 11.3 kg/cm. ESCs are responsible for spinning the motors at the speed requested by the Pixhawk. For our motors' ESCs, we used the Phoenix ICE 50 [29], which has 34 volts max input and 5 amps output. The ESCs need to be calibrated so that they know the minimum and maximum PWM values that the flight controller will send.

2.4 Power Supply

We connected four ZIPPY Flightmax 5S1P batteries [30] in parallel using the Hobby King Quadcopter power distribution boards [31]. As the name suggests, power distribution boards distributed the power on our quad tiltrotor and gave us a tidy way to connect our batteries with the ESCs. The capacity of the battery is 3000mAh and the voltage is 18.5V. With the 20C discharge rate, each battery can output a maximum current up to 60A for 3 minutes. So, our power supply has at least 12 minutes endurance.

While powering the Pixhawk, the Pixhawk power module will provide a steady 5V to the Pixhawk and enable the Pixhawk to measure the current and voltage of the batteries. The operating voltage of our servos is 7.4V, so we used a BEC (Battery Eliminator Circuit) to draw voltage from the motor batteries and drop the operating voltage to a level that is suitable for our servos. For our BEC, we used the Castle Creations CC Bec Pro [32]. Finally, we powered the ESCs directly from our batteries. Figure 2.3 shows the wiring of our quad tiltrotor's power supply.

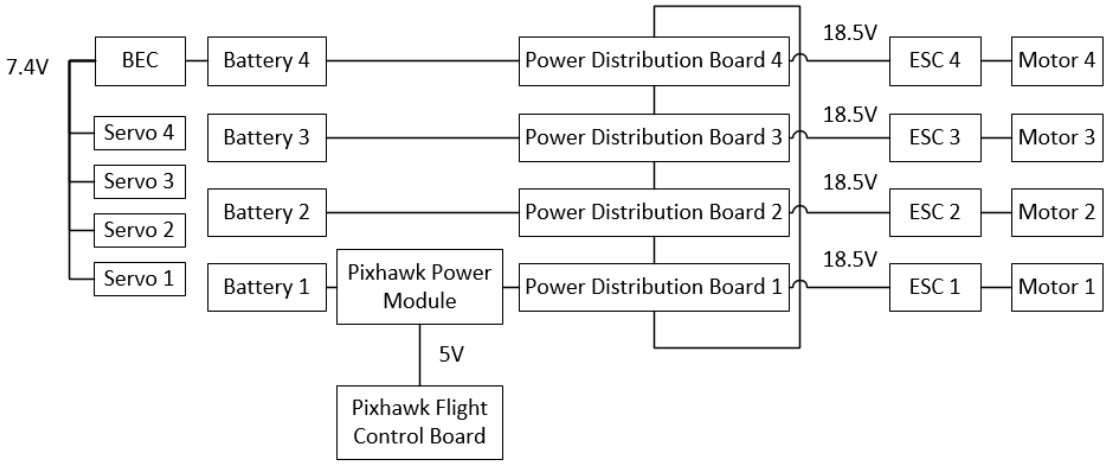

Figure 2.3: The power supply of our quad tiltrotor.

Chapter 3

Dynamic Model

In this chapter, we derive the dynamic equations for the quad tiltrotor in the Earth-fixed frame using the method found in [33].

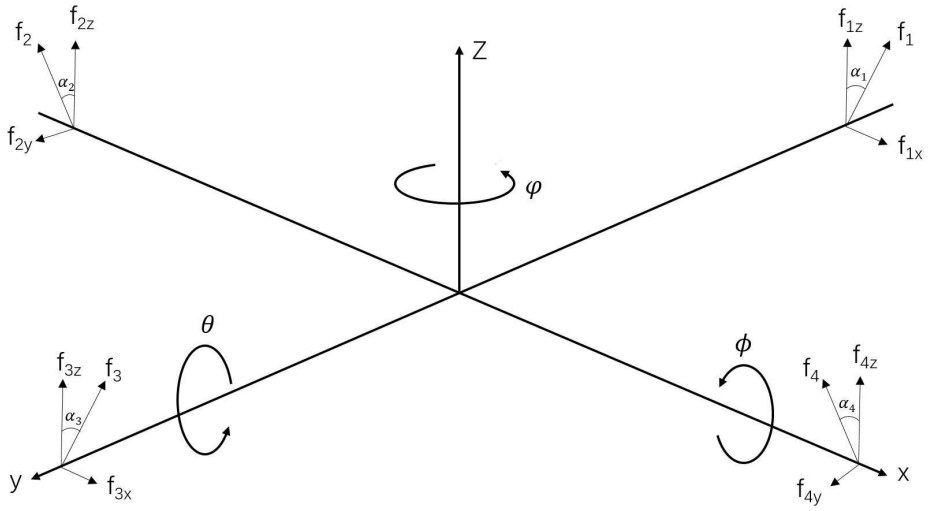

Figure 3.1: Force diagram of our quad tiltrotor.

3.1 Rotation Matrix

There are two coordinate systems: the geography coordinate system (Earth Frame) and the carrier coordinate system (Body Frame). The geography coordinate system refers to the northeast day (ENU) coordinate system on Earth, while the carrier coordinate system is our vehicle-fixed frame. When we control the quad tiltrotor, one problem that concerns us is the change of the vehicle-fixed frame about the Earth-fixed frame. So, we usually use the rotation matrix to transform the geography coordinate system to the carrier coordinate system (as depicted in Figure 3.1). The position of the vehicle is denoted by the 3D vector $\xi = [x, y, z]^T$ and the attitude is denoted by $\eta = [\phi, \theta, \varphi]^T$ where $[x, y, z]$ denotes the quad tiltrotor displacement in three axes and $[\phi, \theta, \varphi]$ denotes the roll, pitch and yaw angle of the quad tiltrotor.

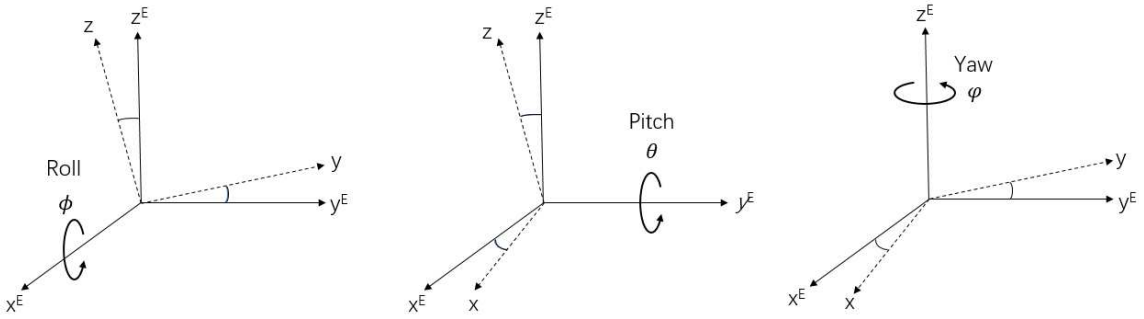

Figure 3.2: Rotation for each axis.

First, we calculate the rotation matrix from the Earth-fixed frame to the vehicle-fixed frame. Figure 3.2 shows the rotation sequence and each of them has its rotation matrix given as follows:

$$R_x = \begin{bmatrix} 1 & 0 & 0 \\ 0 & cos\phi & -sin\phi \\ 0 & sin\phi & cos\phi \end{bmatrix} \tag{3.1}$$

$$R_y = \begin{bmatrix} cos\theta & 0 & sin\theta \\ 0 & 1 & 0 \\ -sin\theta & 0 & cos\theta \end{bmatrix} \tag{3.2}$$

$$R_z = \begin{bmatrix} cos\varphi & -sin\varphi & 0 \\ sin\varphi & cos\varphi & 0 \\ 0 & 0 & 1 \end{bmatrix} \tag{3.3}$$

Then we can get the transformation matrix

$$\begin{aligned} R &= (R_z R_y R_x)^{-1} \\ &= \begin{bmatrix} cos\varphi cos\theta & cos\theta sin\varphi & -sin\theta \\ cos\varphi sin\theta sin\phi - cos\phi sin\varphi & cos\varphi cos\phi + sin\varphi sin\theta sin\phi & cos\theta sin\phi \\ sin\varphi sin\phi + cos\varphi cos\phi sin\theta & cos\phi sin\varphi sin\theta - cos\varphi sin\phi & cos\phi cos\theta \end{bmatrix} \end{aligned} \tag{3.4}$$

3.2 Motion Equations

Next, we define the generalized coordinates $q = [\xi, \eta]^T$. So, the Lagrangian can be defined as

$$L(q, \dot{q}) = T_{trans} + T_{rot} - U \tag{3.5}$$

where $U = mgz$ is the gravitational energy, $T_{trans} = (\frac{1}{2})m\dot{\xi}^T\dot{\xi}$ is the translational kinetic energy and $T_{rot} = (\frac{1}{2})\omega^T I\omega$ is the rotational kinetic energy. I is the moment of inertia matrix of the quad tiltrotor which is assumed to keep only three principle moments due to the symmetry of mass distribution, i.e.,

$$I = \begin{bmatrix} I_{xx} & 0 & 0 \\ 0 & I_{yy} & 0 \\ 0 & 0 & I_{zz} \end{bmatrix}, \tag{3.6}$$

m is the mass of the quad tiltrotor. ω is the angular velocity of the quad tiltrotor defined in the Earth-fixed frame. While the roll angle rate $\dot{\phi}$ is defined in the Earth-fixed frame, the pitch angle rate $\dot{\theta}$ is defined in the vehicle-fixed frame, which is obtained by rotating the Earth-fixed frame about the x axis by the roll angle ϕ. The yaw angle rate $\dot{\varphi}$ is defined in the vehicle-fixed frame, which is obtained by rotating the Earth-fixed frame about the x axis by the roll angle ϕ and then the y axis by the pitch angle θ. We derived the transformation matrix of the angular velocity using the method found in [34]:

$$\omega = \dot{\phi}\begin{bmatrix}1\\0\\0\end{bmatrix} + \dot{\theta}R_x^{-1}\begin{bmatrix}0\\1\\0\end{bmatrix} + \dot{\varphi}(R_yR_x)^{-1}\begin{bmatrix}0\\0\\1\end{bmatrix} = \begin{bmatrix}\dot{\phi} - \dot{\varphi}sin\theta\\ \dot{\theta}cos\phi + \dot{\varphi}sin\phi cos\theta\\ -\dot{\theta}sin\phi + \dot{\varphi}cos\phi cos\theta\end{bmatrix} = W_v\dot{\eta} \quad (3.7)$$

So,

$$W_v = \begin{bmatrix}1 & 0 & -sin\theta\\ 0 & cos\phi & sin\phi cos\theta\\ 0 & -sin\phi & cos\phi cos\theta\end{bmatrix} \quad (3.8)$$

Then we define $J = J(\eta) = W_v^T I W_v$ to simplify the rotational kinetic energy T_{rot}, which makes $T_{rot} = (\frac{1}{2})\dot{\eta}^T J\dot{\eta}$.

As for the force analysis, we define the external forces

$$F = \begin{bmatrix}F_x\\F_y\\F_z\end{bmatrix} = \begin{bmatrix}f_{1x} + f_{3x}\\ f_{2y} + f_{4y}\\ f_{1z} + f_{2z} + f_{3z} + f_{4z}\end{bmatrix} \quad (3.9)$$

where f_{ij} are the thrust components generated by the motor i in the j axis, and

torques

$$\tau = \begin{bmatrix} \tau_\phi \\ \tau_\theta \\ \tau_\varphi \end{bmatrix} = \begin{bmatrix} (f_{1z} - f_{3z})l \\ (f_{4z} - f_{2z})l \\ (f_{3x} - f_{1x})l + (f_{2y} - f_{4y})l \end{bmatrix} \tag{3.10}$$

where l is the moment arm between opposing propellers and

$$f_{1x} = f_1 sin\alpha_1,\ f_{1z} = f_1 cos\alpha_1,\ f_{2y} = f_2 sin\alpha_2,\ f_{2z} = f_2 cos\alpha_2 \tag{3.11}$$

$$f_{3x} = f_3 sin\alpha_3,\ f_{3z} = f_3 cos\alpha_3,\ f_{4y} = f_4 sin\alpha_4,\ f_{4z} = f_4 cos\alpha_4 \tag{3.12}$$

and α_1, α_2, α_3, α_4 are the angles of each of the rotor gimbals.

Finally, we can write the Euler-Lagrange equation of our quad tiltdrotor

$$\frac{d}{dt}\frac{\partial L}{\partial \dot{q}} - \frac{\partial L}{\partial q} = \begin{bmatrix} F_\xi \\ \tau \end{bmatrix} \tag{3.13}$$

where $F_\xi = RF$ is the external force in the Earth-fixed frame.

Thus, we can get the dynamic equations of our quad tiltrotor

$$m\ddot{\xi} + \begin{bmatrix} 0 \\ o \\ mg \end{bmatrix} = RF \tag{3.14}$$

$$J\ddot{\eta} + C(\eta, \dot{\eta})\dot{\eta} = \tau \tag{3.15}$$

where $C(\eta, \dot{\eta}) = \dot{J} - (\frac{1}{2})\frac{\partial}{\eta}(\dot{\eta}^T J)$ is the Coriolis term. Let us rewrite the equations as

follows:

$$\begin{bmatrix} \ddot{x} \\ \ddot{y} \\ \ddot{z} \end{bmatrix} = \frac{1}{m} R \begin{bmatrix} F_x \\ F_y \\ F_z \end{bmatrix} - \begin{bmatrix} 0 \\ 0 \\ g \end{bmatrix} \tag{3.16}$$

$$\begin{bmatrix} \ddot{\phi} \\ \ddot{\theta} \\ \ddot{\varphi} \end{bmatrix} = J^{-1}(\begin{bmatrix} \tau_\phi \\ \tau_\theta \\ \tau_\varphi \end{bmatrix} - C(\eta, \dot{\eta}) \begin{bmatrix} \dot{\phi} \\ \dot{\theta} \\ \dot{\varphi} \end{bmatrix}) \tag{3.17}$$

Chapter 4

Control Scheme

4.1 Control Plant

In our control experiment, the control objective is the attitude of our quad tiltrotor including roll, pitch and yaw angles. As we fixed the quad tiltrotor bottom to a spherical bearing, we did not need to consider the displacement in the x, y and z axes. So, we only kept (3.17) as the dynamic equation of our plant. By changing the RPM of four motors and the angle of four servos, we could produce the required torques to achieve the target attitude.

4.2 Feedback Linearization

The control plant of our quad tiltrotor is nonlinear and complex. To apply linear control laws, we used the feedback linearization method found in [35] and [36] to simplify our control model.

We applied the feedback linearizion control law

$$\begin{bmatrix} \tau_\phi \\ \tau_\theta \\ \tau_\varphi \end{bmatrix} = J \begin{bmatrix} r_\phi \\ r_\theta \\ r_\varphi \end{bmatrix} + C(\eta, \dot{\eta}) \begin{bmatrix} \dot{\phi} \\ \dot{\theta} \\ \dot{\varphi} \end{bmatrix} \tag{4.1}$$

to our control system. So, the system becomes

$$\begin{bmatrix} \ddot{\phi} \\ \ddot{\theta} \\ \ddot{\varphi} \end{bmatrix} = \begin{bmatrix} r_\phi \\ r_\theta \\ r_\varphi \end{bmatrix}, \tag{4.2}$$

where $r_a = \begin{bmatrix} r_\phi \\ r_\theta \\ r_\varphi \end{bmatrix}$ represents our virtual inputs.

4.3 Controller Design

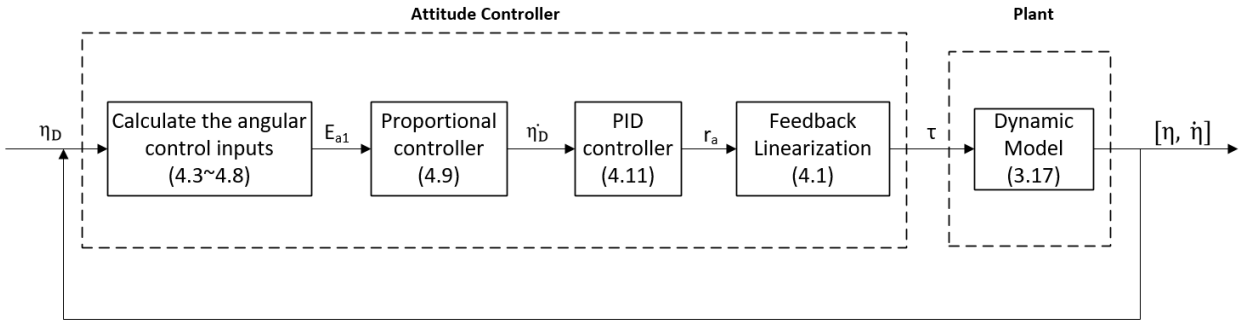

Figure 4.1: The control system diagram.

As Figure 4.1 shows, we deployed the two-level controller found in [37] to generate the desired outputs, which are the substitution inputs used in (4.1). The first level calculates the angular velocity set points with a proportional controller and the second

level is a PID controller.

We designed our controller to track the attitude errors. Let us define the error signals

$$\eta_e = \begin{bmatrix} \phi_e(t) \\ \theta_e(t) \\ \varphi_e(t) \end{bmatrix} = \begin{bmatrix} \phi(t) - \phi_D(t) \\ \theta(t) - \theta_D(t) \\ \varphi(t) - \varphi_D(t) \end{bmatrix}, \tag{4.3}$$

where $\phi_D(t)$, $\theta_D(t)$ and $\varphi_D(t)$ are functions of the desired attitude values, which vary over time.

From many experiments, we can see that the response time of the pitch and roll angles are almost two times faster than the response time of the yaw angle [38]. The rotors only need to change speed a little bit to get enough torque for roll and pitch movement. So, we control the yaw movement separately. We executed the pitch-roll movement first and then the yaw movement [39].

Let us define the z-axis of the desired attitude as a vector z_D and the current z-axis z. They can be calculated by using a rotation matrix from

$$z = R(\eta) \begin{bmatrix} 0 \\ 0 \\ 1 \end{bmatrix}, z_D = R(\eta_D) \begin{bmatrix} 0 \\ 0 \\ 1 \end{bmatrix} \tag{4.4}$$

To make the z_D and z coincide, we got the vector of rotation axis z_e by calculating the cross product of z_D and z

$$z_e = z \times z_D \tag{4.5}$$

while the rotation angle κ_e is

$$\kappa_e = arccos \frac{z_D z}{|z_D||z|} \tag{4.6}$$

So, axis z needs to revolve around z_e for κ_e degrees to achieve z_D as the first step.

We multiply κ_e by z_e to get the control inputs.

$$E_a = \kappa_e z_e = \begin{bmatrix} E_{a\phi}(t) \\ E_{a\theta}(t) \\ E_{a\varphi}(t) \end{bmatrix} \tag{4.7}$$

We keep the last two terms of E_a and replace the last with angle error φ_e. When our controller takes E_a as the input, only the pitch and roll controller is doing tracking. Then the yaw control will get involved. This decomposition decouples the controller behaviors to fast response motion and slow response motion.

Then we rearrange the error terms. So the control inputs for our first level controller are

$$E_{a1} = \begin{bmatrix} E_{a\phi}(t) \\ E_{a\theta}(t) \\ \varphi_e(t) \end{bmatrix} \tag{4.8}$$

We applied the control law

$$\dot{\eta}_D = \begin{bmatrix} \dot{\phi}_D(t) \\ \dot{\theta}_D(t) \\ \dot{\varphi}_D(t) \end{bmatrix} = \begin{bmatrix} k_\phi E_{a\phi}(t) \\ k_\theta E_{a\theta}(t) \\ k_\varphi \varphi_e(t) \end{bmatrix}, \tag{4.9}$$

where k_ϕ, k_θ and k_φ are positive definite control gains.

Let us define the error of angular rates as

$$\dot{\eta}_e = \begin{bmatrix} \dot{\phi}_e(t) \\ \dot{\theta}_e(t) \\ \dot{\varphi}_e(t) \end{bmatrix} = \begin{bmatrix} \dot{\phi}(t) - \dot{\phi}_D(t) \\ \dot{\theta}(t) - \dot{\theta}_D(t) \\ \dot{\varphi}(t) - \dot{\varphi}_D(t) \end{bmatrix} \tag{4.10}$$

The control law is as follows:

$$r_a = \begin{bmatrix} r_\phi \\ r_\theta \\ r_\varphi \end{bmatrix} = P_{a2} \begin{bmatrix} \dot{\phi}_e(t) \\ \dot{\theta}_e(t) \\ \dot{\varphi}_e(t) \end{bmatrix} + D_a \begin{bmatrix} \ddot{\phi}_e(t) \\ \ddot{\theta}_e(t) \\ \ddot{\varphi}_e(t) \end{bmatrix} + I_a \begin{bmatrix} \phi_e(t) \\ \theta_e(t) \\ \varphi_e(t) \end{bmatrix}. \tag{4.11}$$

4.4 Simulation

Table 4.1: Simulation Parameters.

Sampling time	Δt	1ms
Principle moments of inertia	I_x	$0.2kg \bullet m^2$
	I_y	$0.2kg \bullet m^2$
	I_z	$0.4kg \bullet m^2$
Control gains	k_ϕ	30
	k_θ	30
	k_φ	60
	P_a	10
	I_a	50
	D_a	50

We ran the simulation of the control model given in section 4.3 with MATLAB. Since η_D is near to the origin, we could ignore the Coriolis Force item. So, we simplified the dynamical model (3.17) as follows to reduce the computational expense of the highly nonlinear (4.1).

$$\begin{bmatrix} \ddot{\phi} \\ \ddot{\theta} \\ \ddot{\varphi} \end{bmatrix} = J^{-1} \begin{bmatrix} \tau_\phi \\ \tau_\theta \\ \tau_\varphi \end{bmatrix} \tag{4.12}$$

Then the feedback linearizion control law becomes:

$$\begin{bmatrix} \tau_\phi \\ \tau_\theta \\ \tau_\varphi \end{bmatrix} = J \begin{bmatrix} r_\phi \\ r_\theta \\ r_\varphi \end{bmatrix} \tag{4.13}$$

Figures 4.2, 4.4 and 4.6 show the closed-loop initial perturbation rejection of the attitude control system. Figures 4.8, 4.10 and 4.12 shows the closed-loop tracking response of the attitude control system. Figures 4.3, 4.5, 4.7, 4.9, 4.11 and 4.13 shows the torques we need to achieve the desired attitude. We can see that the response is fast and the system is stable. The simulation parameters are laid out in table 4.1.

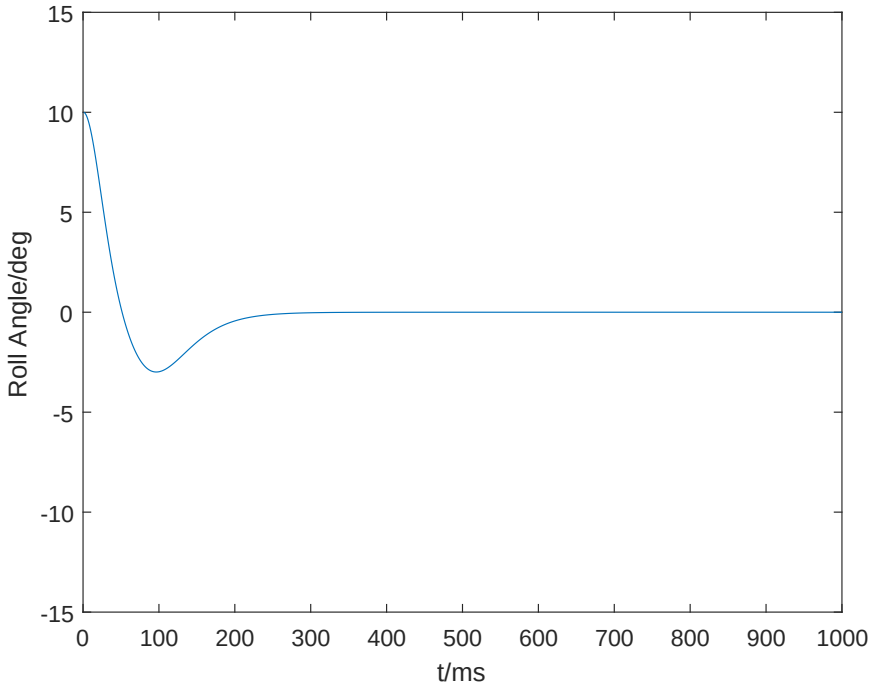

Figure 4.2: The initial perturbation rejection of roll.

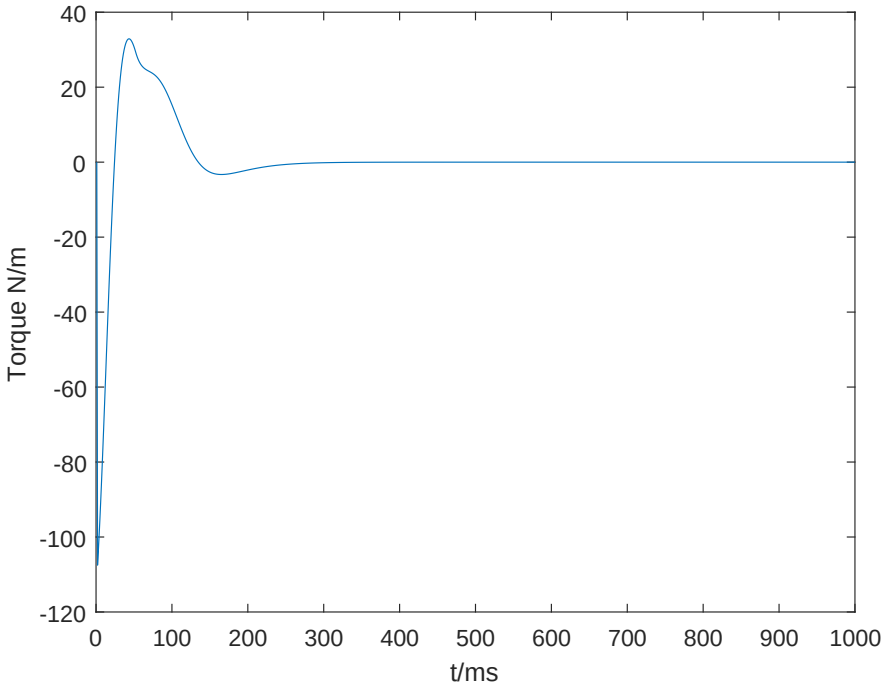

Figure 4.3: The generated torque for rolling.

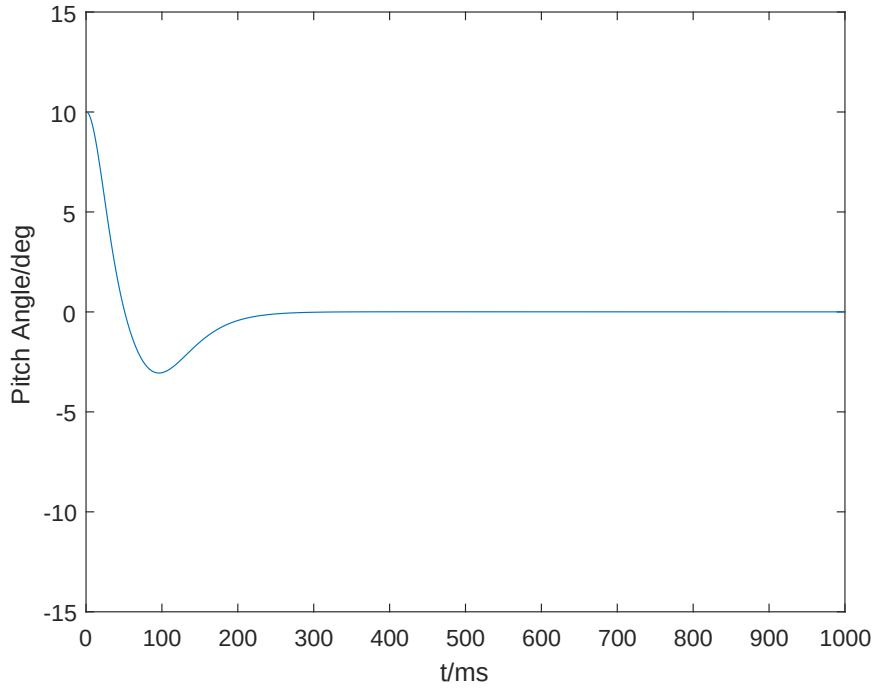

Figure 4.4: The initial perturbation rejection of pitch.

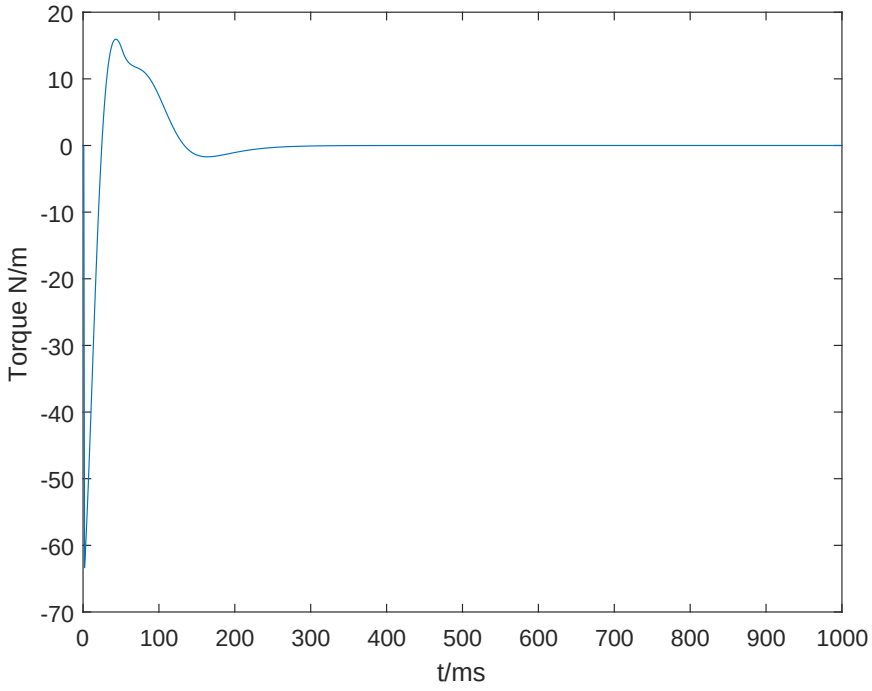

Figure 4.5: The generated torque for pitching.

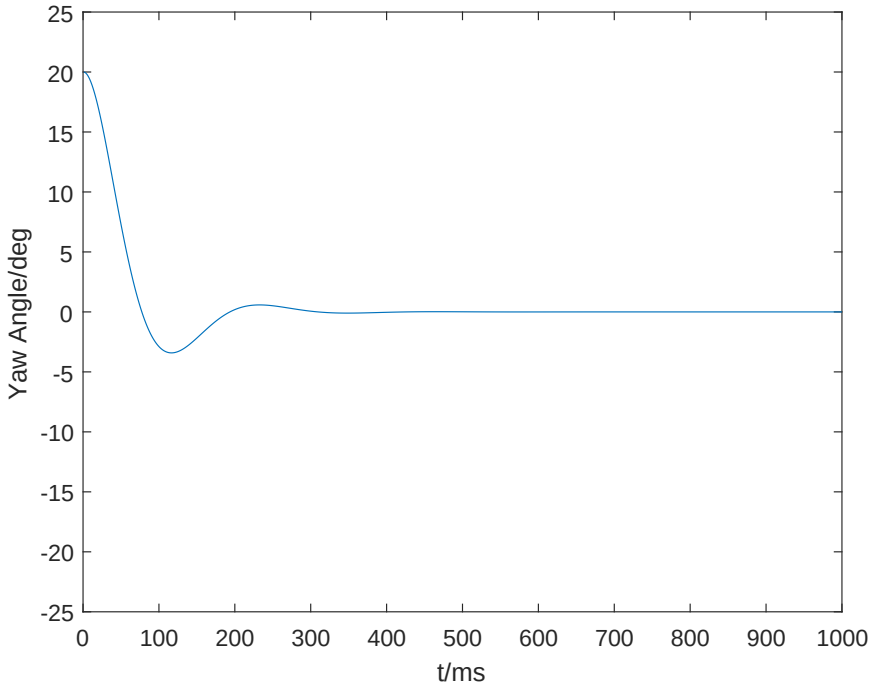

Figure 4.6: The initial perturbation rejection of yaw.

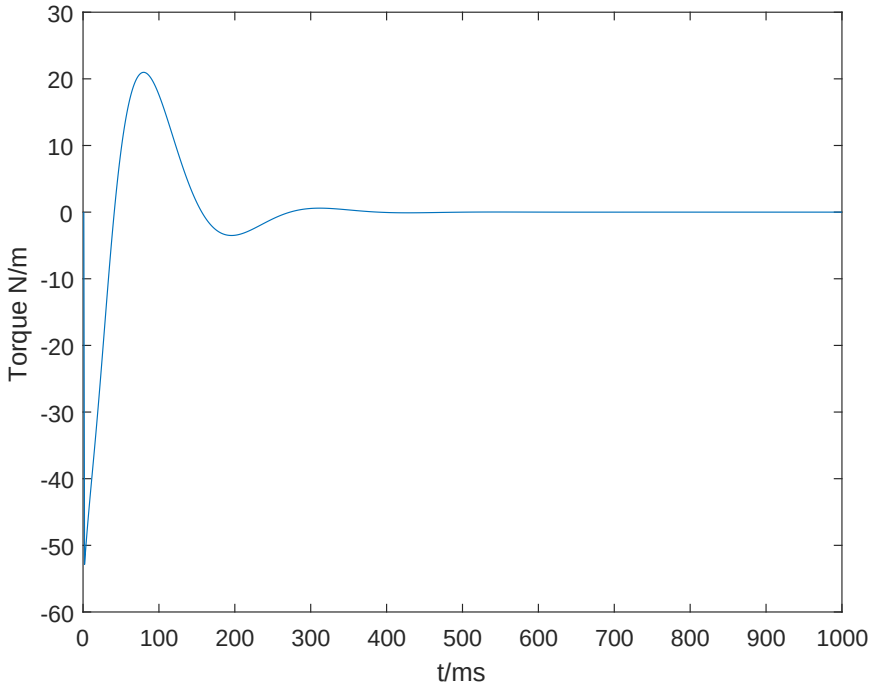

Figure 4.7: The generated torque for yawing.

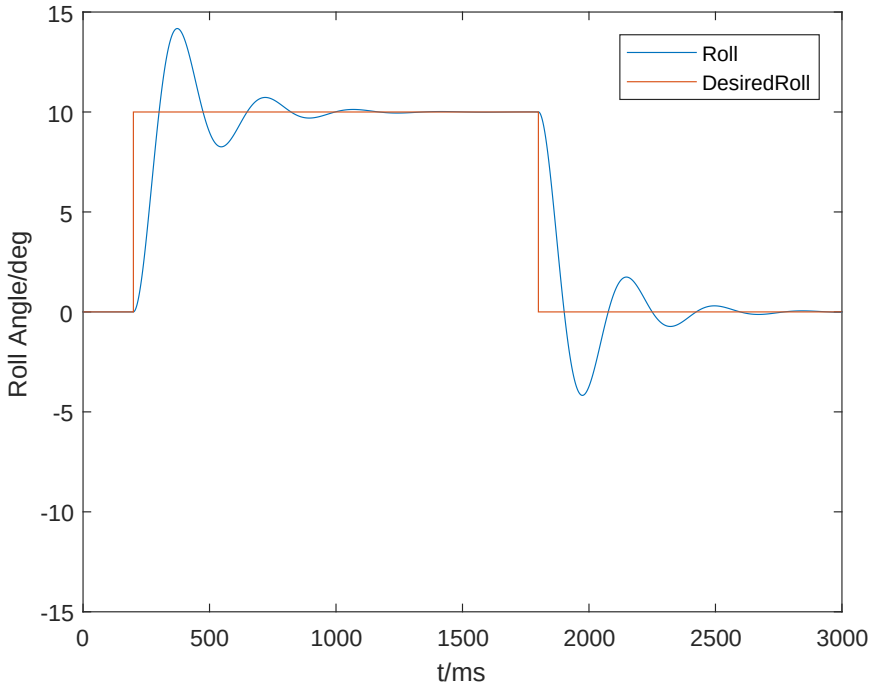

Figure 4.8: The roll inputs and responses.

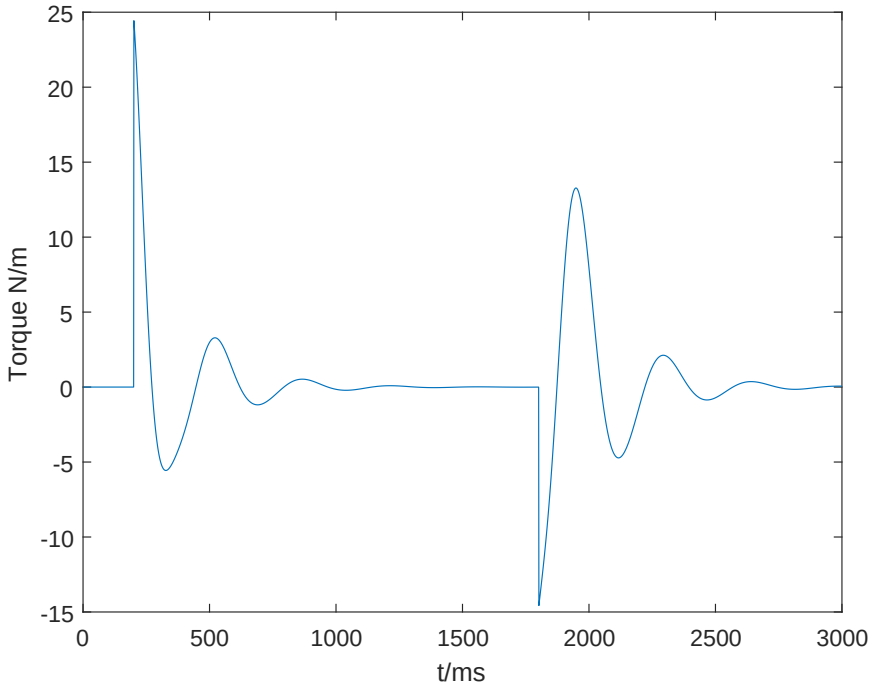

Figure 4.9: The generated torque for rolling.

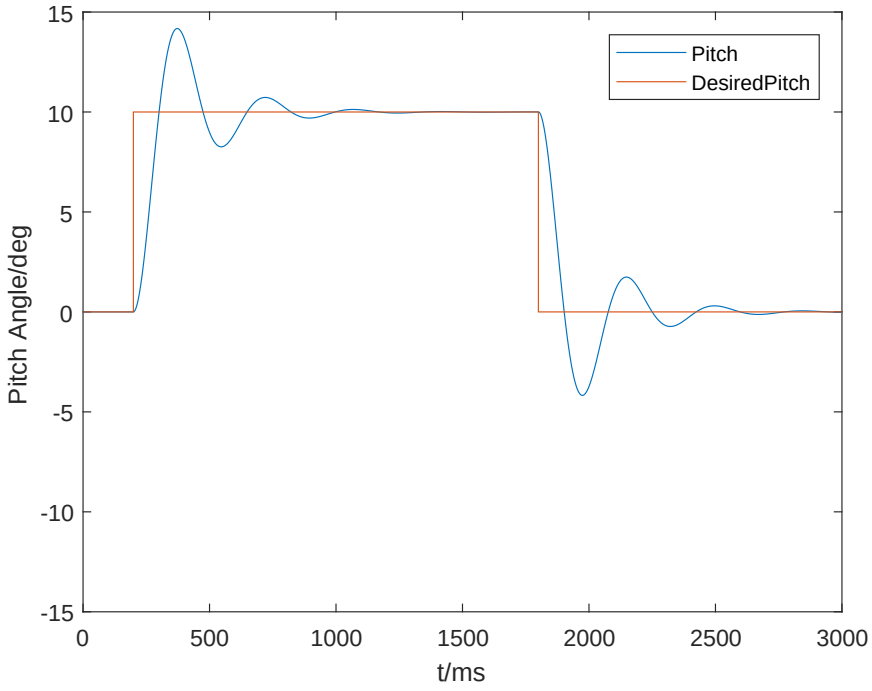

Figure 4.10: The pitch inputs and responses.

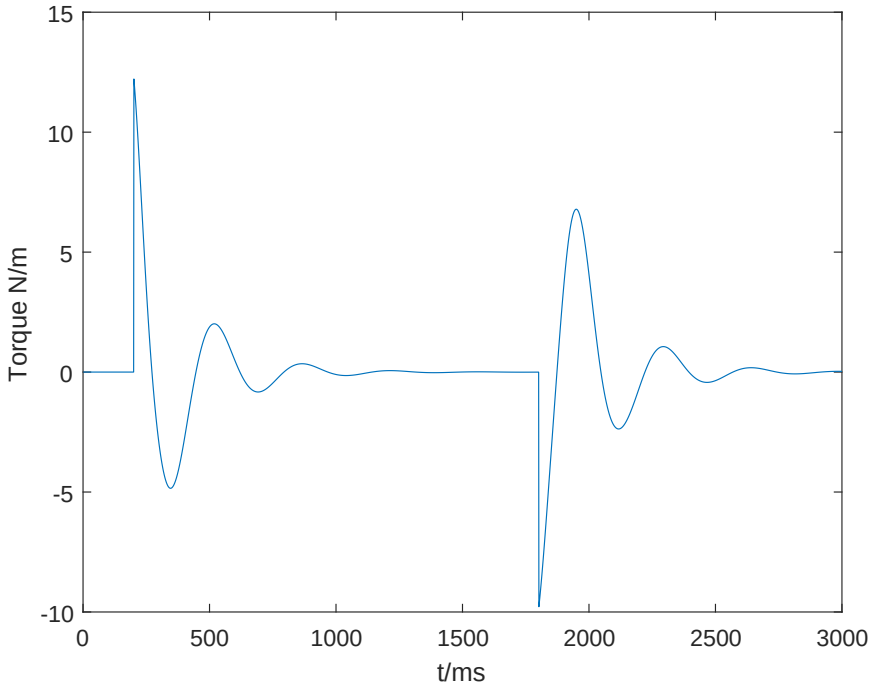

Figure 4.11: The generated torque for pitching.

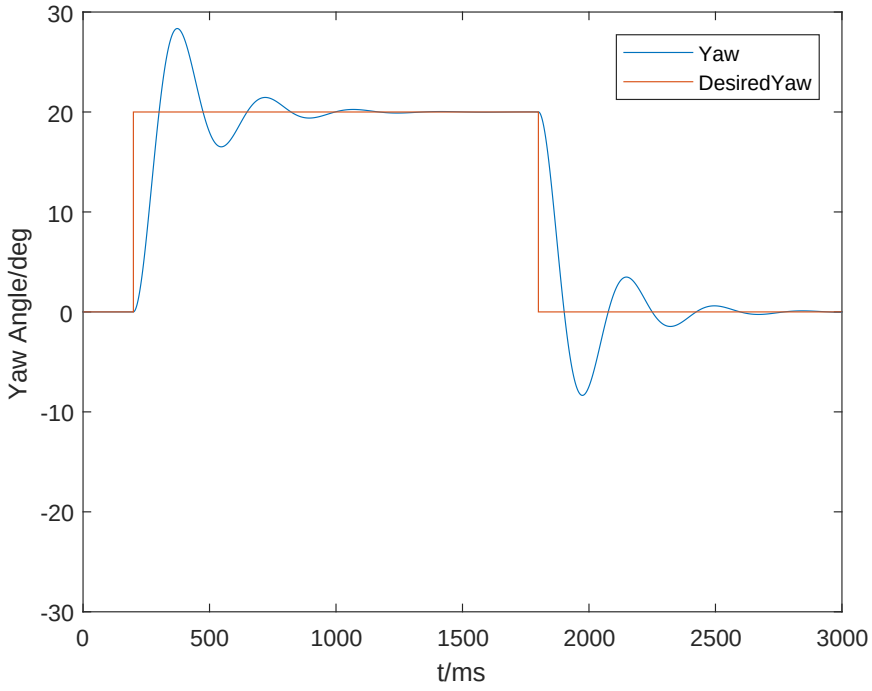

Figure 4.12: The yaw inputs and responses.

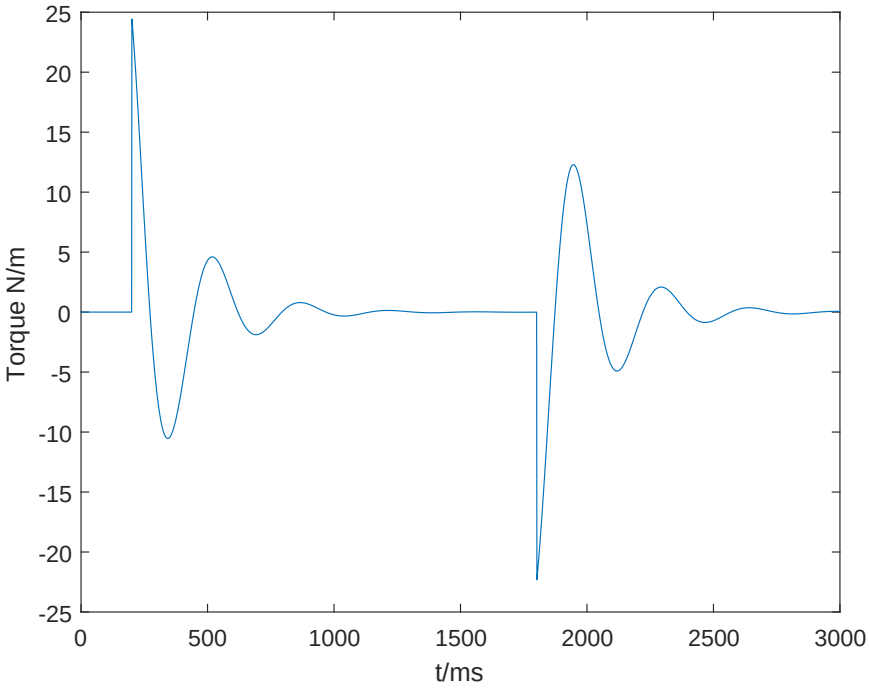

Figure 4.13: The generated torque for yawing.

Chapter 5

Implementation

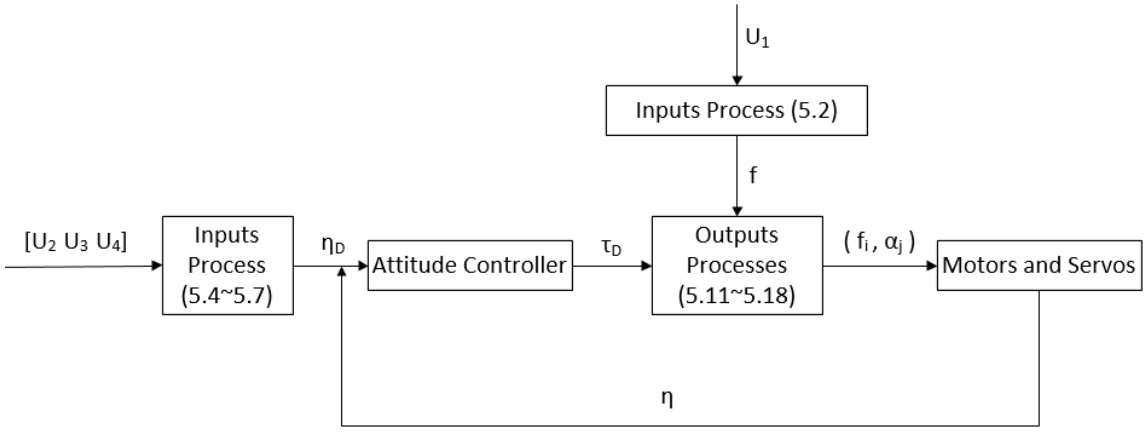

Figure 5.1: The block diagram of implementation.

5.1 Inputs Process

We use a transmitter with four sticks to control the quad tiltrotor in experiments where the four inputs are defined as U_1, U_2, U_3 and U_4. In this study, U_1 controls the thrust; U_2, U_3 control the roll and pitch angles; and U_4 controls the yaw angle rate.

First, we rescale the range of transmitters which means $U_1 \in [0, 1]$, $U_2 \in [-1, 1]$,

$U_3 \in [-1, 1]$ and $U_4 \in [-1, 1]$. Note that the thrust of a propeller is determined by

$$f = \frac{1}{2}\rho C\omega^2, \tag{5.1}$$

where ρ is the air density, C is the lift coefficient of the propeller and ω is the angular rate of the propeller [40]. We define the desired initial thrust generated by each propeller as

$$f = k_t U_1, \tag{5.2}$$

where k_t is the coefficient of the thrust input U_1. So, the initial angular rate of each propeller is

$$\omega = (\frac{2k_t}{\rho C})^{\frac{1}{2}} U_1^{\frac{1}{2}} \tag{5.3}$$

When $U_1 > 0$ and $U_2, U_3, U_4 = 0$, the four motors will have the same rotation speed in proportion to the radication of U_1. Thus the attitude will not change, which means our control system presented in Chapter 4 is independent of U_1.

Then we can get the attitude set points and thrust value by inputs processes as follows:

$$\phi_D = k_\phi U_2 \tag{5.4}$$

$$\theta_D = k_\theta U_3 \tag{5.5}$$

$$\dot{\varphi}_D = k_\varphi U_4 \tag{5.6}$$

So, the desired yaw angle is

$$\varphi_D = \int k_\varphi U_4 dt \tag{5.7}$$

Since we calculated the attitude setpoints above, we can compute the desired torque using the attitude controller derived in Chapter 4, combined with the actual

attitude data.

5.2 Outputs Process

Using the attitude controller presented in Figure 4.1, we get the desired torques τ_φ, τ_θ and τ_ϕ. The next step is calculating the desired thrust of each propeller and the desired angle of each gimbal. Let us define the thrust generated by each motor as $f_i, i = 1, 2, 3, 4$ and the angle of each servo as $\alpha_j, j = 1, 2, 3, 4$. To simplify the outputs we define

$$\alpha_1 = -\alpha_3 \tag{5.8}$$

$$\alpha_2 = -\alpha_4 \tag{5.9}$$

$$|\alpha_1| = |\alpha_2| = |\alpha_3| = |\alpha_4| \tag{5.10}$$

When we combine the initial thrust determined by U_1 and the desired torques calculated by the attitude controller, we get the following outputs:

$$f_1 = f + \frac{\tau_\phi}{l} \tag{5.11}$$

$$f_2 = f - \frac{\tau_\theta}{l} \tag{5.12}$$

$$f_3 = f - \frac{\tau_\phi}{l} \tag{5.13}$$

$$f_4 = f + \frac{\tau_\theta}{l} \tag{5.14}$$

$$\alpha_1 = -arcsin\frac{\tau_\varphi}{4fl} \tag{5.15}$$

$$\alpha_2 = arcsin\frac{\tau_\varphi}{4fl} \tag{5.16}$$

$$\alpha_3 = arcsin\frac{\tau_\varphi}{4fl} \tag{5.17}$$

$$\alpha_4 = -arcsin\frac{\tau_\varphi}{4fl} \tag{5.18}$$

Finally, because the pulse width is proportional to the radication of the thrusts and the angles, we turned the eight outputs to PWM signals in order to control the rotation speed of the motors and the angles of the servos using the code found in [41].

Chapter 6

Experiments

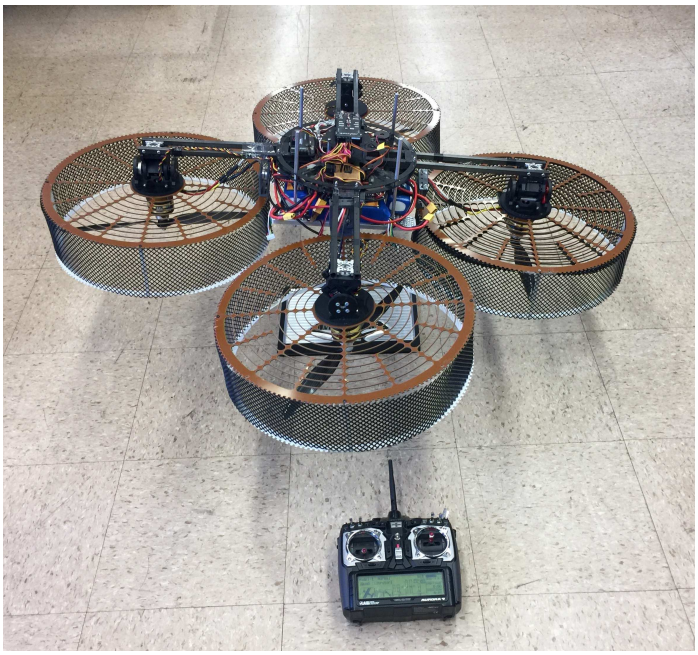

Figure 6.1: The environment of our experiment.

6.1 Experiment Objective

We designed an experiment for our quad tiltrotor attitude controller that we presented in Chapter 4. We used the transmitter to input the reference roll, pitch and

yaw angles of our quad tiltrotor. As we moved the transmitter sticks, our quad tiltrotor would reach the corresponding attitude by changing the rotation speed of the propellers and the angles of the gimbals. The purpose of this experiment was to find control parameters that would minimize the control errors and give students a better understanding of PID controllers.

6.2 Experimental Procedure

The components of this experiment include a transmitter, our quad tiltrotor, a test revolve stand (Figure 6.2) and ground control systems. First, we fixed our quadrotor in a revolving stand with a spherical bearing. As the spherical bearing limited the displacement of our quad tiltrotor in all directions, the quad tiltrotor could only make angular rotations after we loosened the bolt. We also needed to make the quad tiltrotor horizontal and have it face north in order to reset the three attitude angles to zero.

Figure 6.2: The test stand.

Next, we connected the Pixhawk board to a computer with a USB cable. Then we downloaded the firmware and calibrated the sensors and transmitters on Mission

Planner. After that, we could write the control parameters into the Pixhawk as Figure 6.3 shows. Details regarding the above operations can be found in [42].

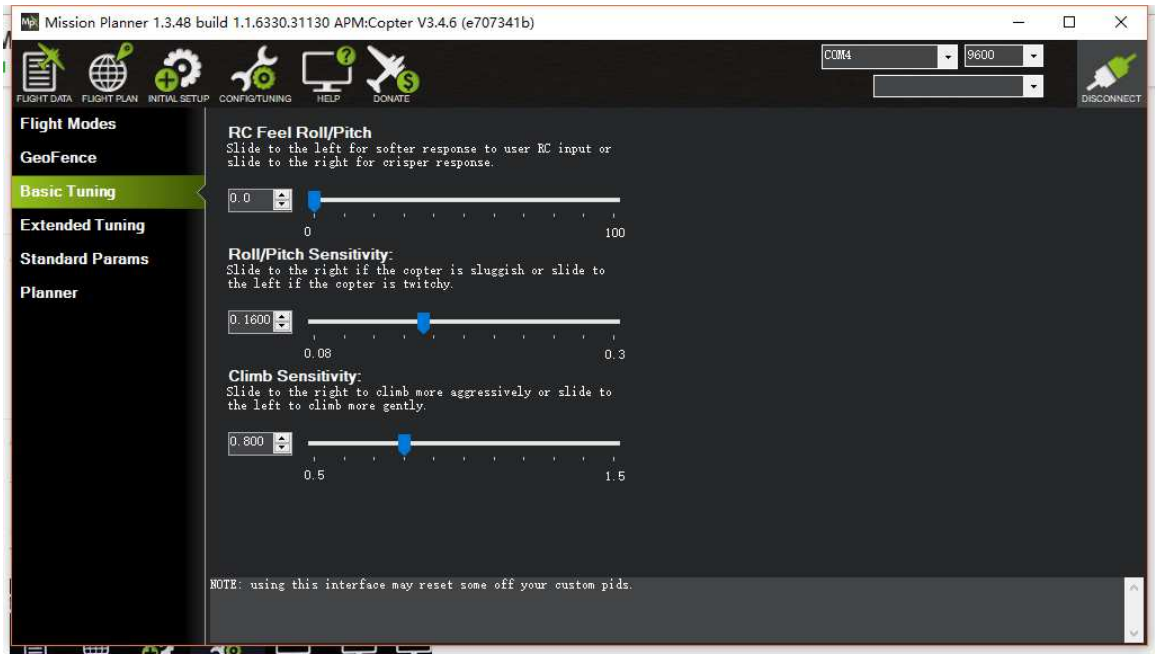

Figure 6.3: The GUI of controller tuning.

Finally, we turned on the quad tiltrotor and the transmitter. Before changing the attitude of our quad tiltrotor, we needed to move the throttle stick to the middle position. As the four motors had the same rotation speed, the quad tiltrotor stayed stable. Then we could move the roll, pitch and yaw stick to change the attitude of our quad tiltrotor. Once we had finished recording our observations, we stopped the propellers by moving the throttle stick to the lowest position.

6.3 Results Analysis

We carried out the experiments described in Section 6.2. Figure 6.4 shows the PID parameters we used. The data of our quad tiltrotor state and transmitter inputs during the experiment were stored in the Pixhawk board as flight logs. As Figure 6.5 shows, we designed a MATLAB GUI to refine and analyze the results. Our GUI

could read the log files, plot the results and set the time span to display the plot in different accuracies.

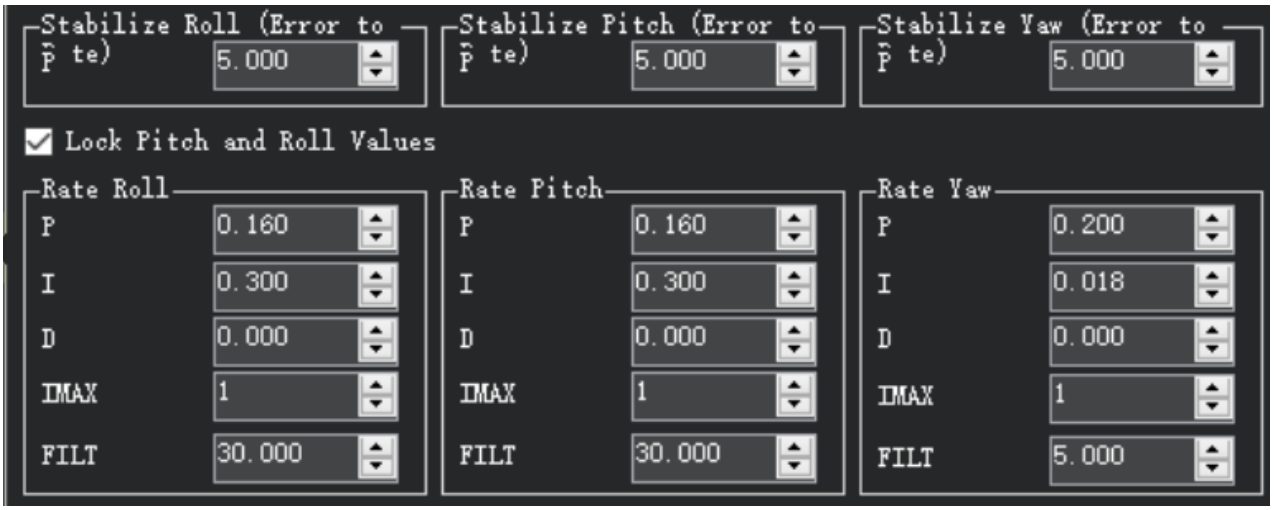

Figure 6.4: The PID parameters of attitude control system.

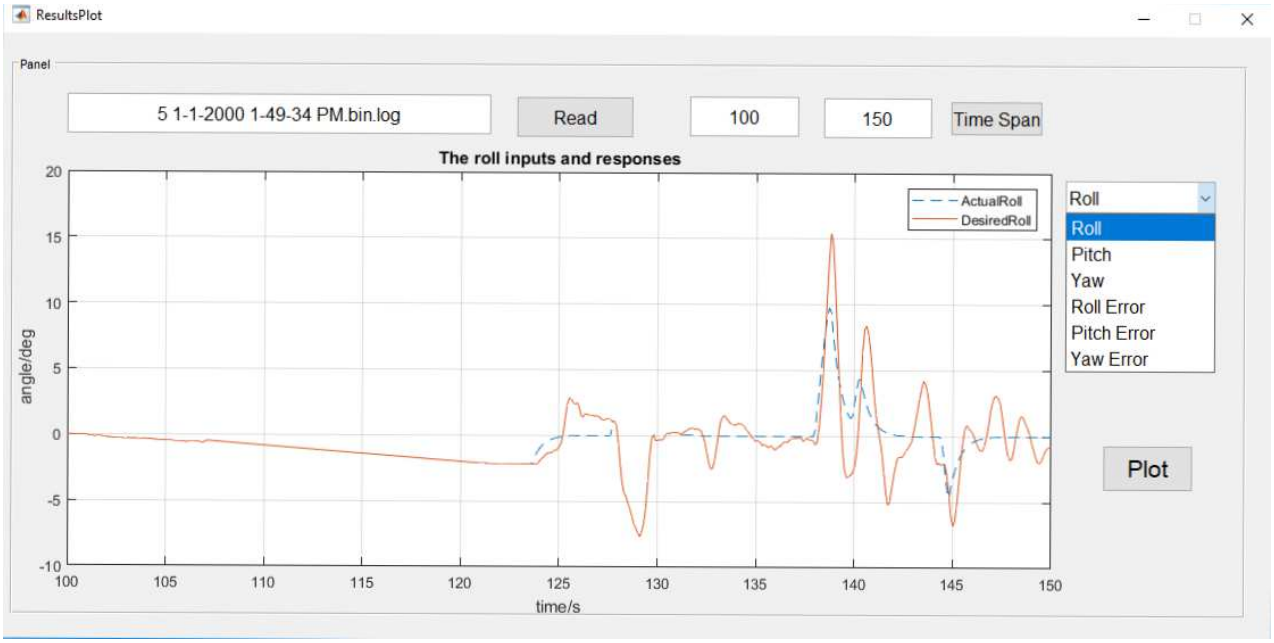

Figure 6.5: The Matlab GUI.

Figures 6.6 through 6.10 show the results of one example experiment. The plots illustrate that our controller works well most of the time. But errors increased significantly around the peak values. That is because our quad tiltrotor cannot reach such large attitude angles.

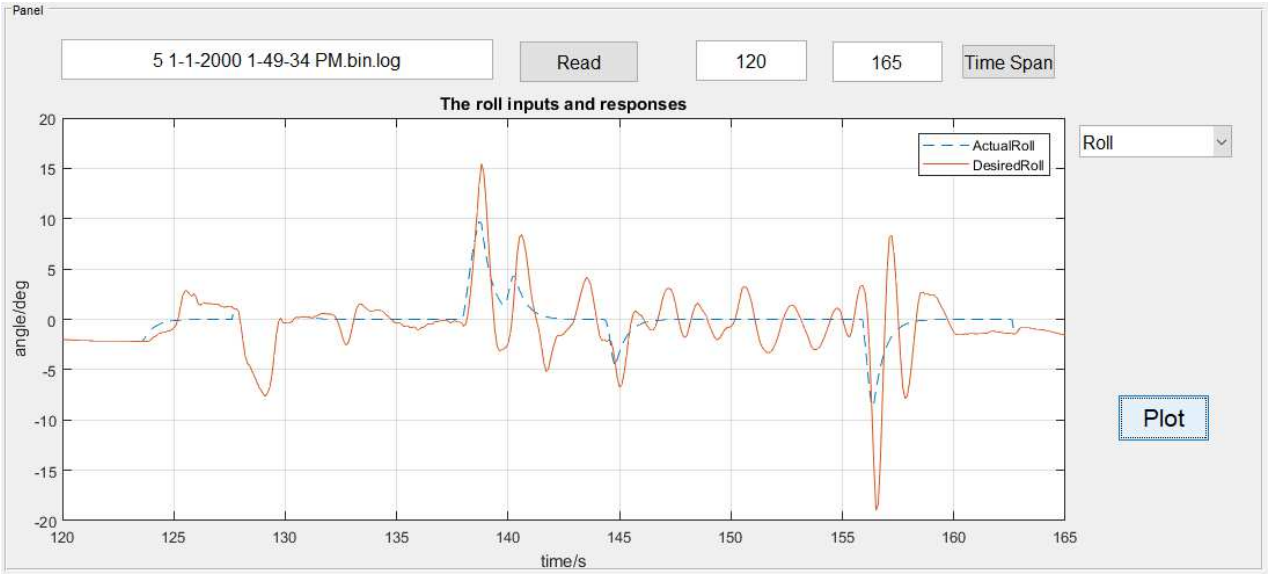

Figure 6.6: The actual and desired roll angle of quad tiltrotor vary over time.

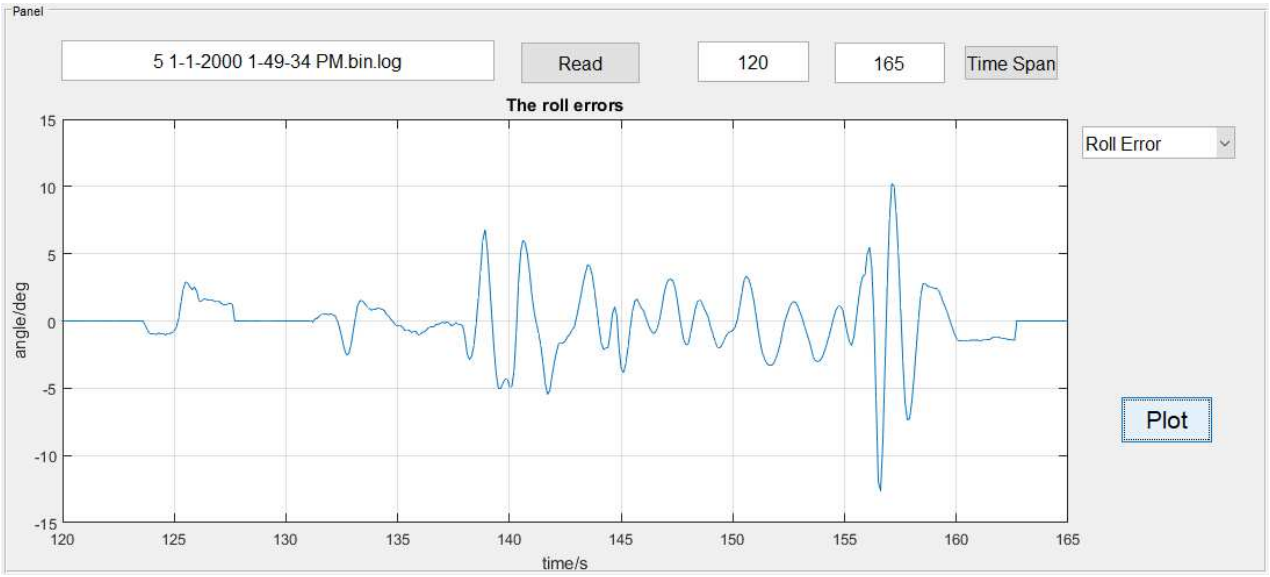

Figure 6.7: The control errors of roll angle.

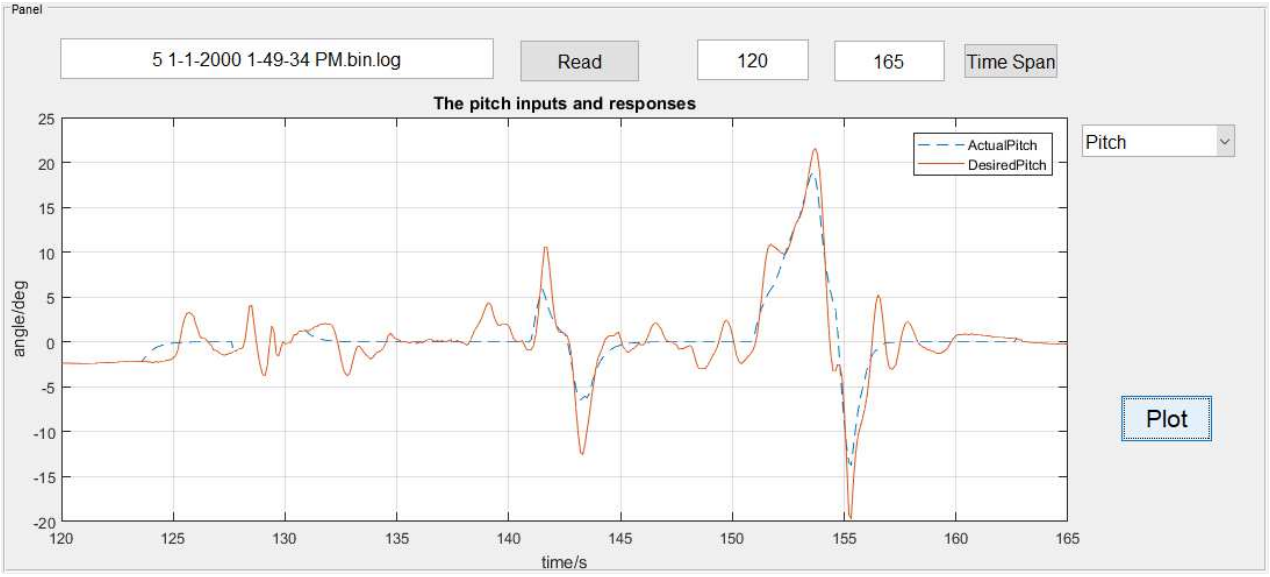

Figure 6.8: The actual and desired pitch angle of quad tiltrotor vary over time.

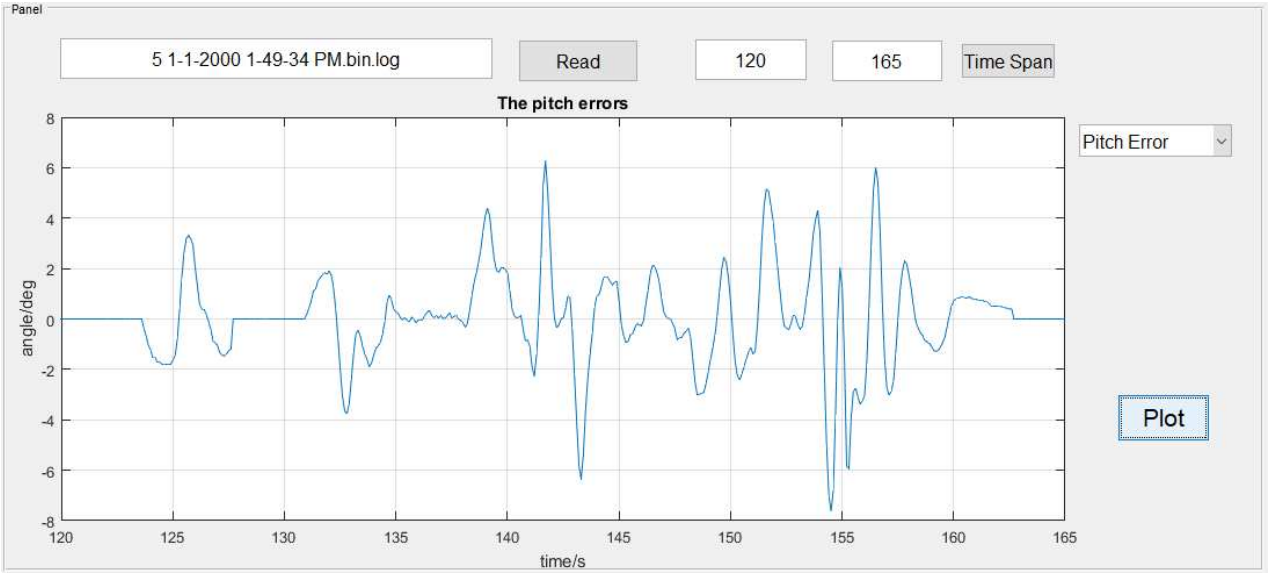

Figure 6.9: The control errors of pitch angle.

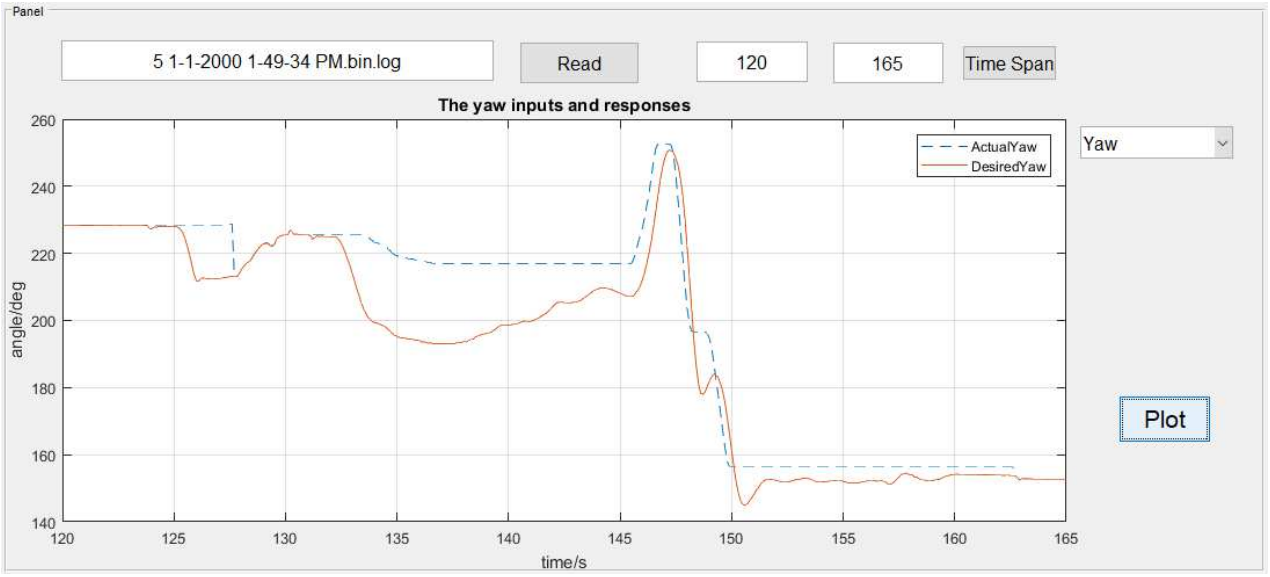

Figure 6.10: The actual and desired yaw angle of quad tiltrotor vary over time.

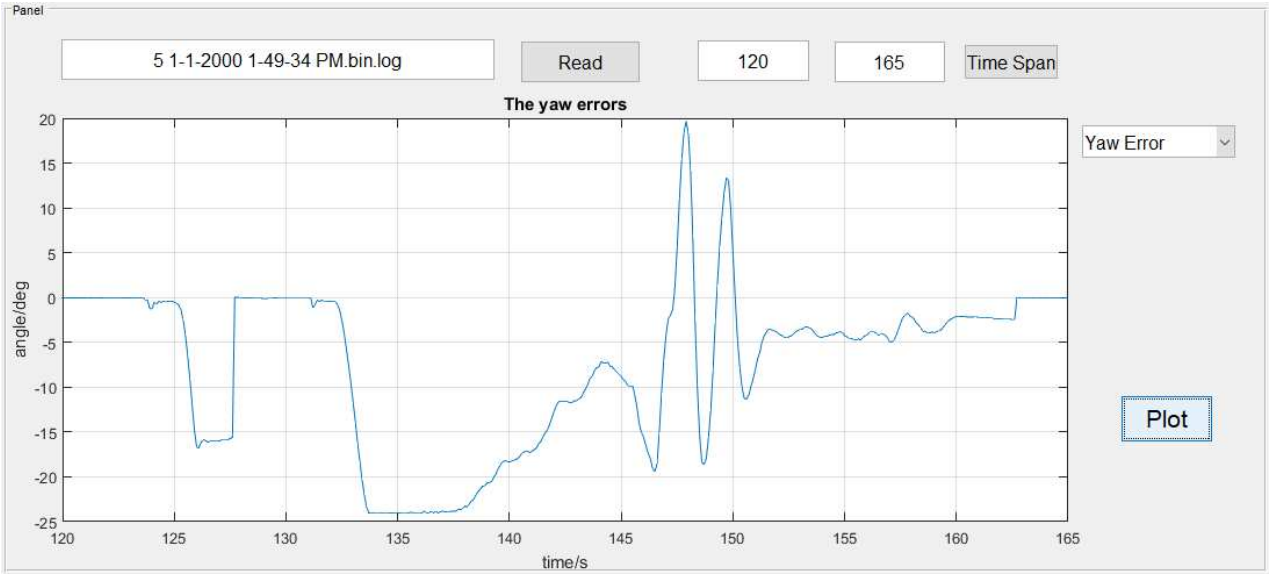

Figure 6.11: The control errors of yaw angle.

Chapter 7

Conclusion and Future Works

7.1 Conclusion

This thesis presents a quad tiltrotor design that can be used as a teaching instrument, especially in control classes. The test stand increases the safety of the instruction and allows students to pay full attention to the design of the attitude controller, which is the most important part of the quad tiltrotor control system. Furthermore, the control strategy has been proven efficient and will enable students to adjust the PID parameters of the controller in a friendly interface. By controlling the pitch, roll and yaw angle of this quadrotor separately, we make it possible to apply multiple control methods for this sytem. The flight log GUI of our control system makes the result analysis much easier.

7.2 Future Works

The next step of this project is to replace the Mission Planner GUI with one that is simpler and more professional. Doing so will make it easier to modify control parameters and analyze results. Then we could propose other control strategies such as

LQR and backstepping. Ultimately, we would do well to make a more comprehensive evaluation of the attitude controller. For instance, we ought to take into consideration the robustness of the controller. Future investigations like these will enhance the practicability of the controller that we designed.

Bibliography

[1] G. Hoffmann, D. G. Rajnarayan, S. L. Waslander, D. Dostal, J. S. Jang and C. J. Tomlin, "The Stanford testbed of autonomous rotorcraft for multi agent control (STARMAC)," The 23rd Digital Avionics Systems Conference (IEEE Cat. No.04CH37576), 2004, pp. 12.E.4-121-10 Vol.2.

[2] A. Azzam and Xinhua Wang, "Quad rotor arial robot dynamic modeling and configuration stabilization," 2010 2nd International Asia Conference on Informatics in Control, Automation and Robotics (CAR 2010), Wuhan, 2010, pp. 438-444.

[3] H. Liu, Y. Bai, G. Lu and Y. Zhong, "Brief Paper - Robust attitude control of uncertain quadrotors," in IET Control Theory & Applications, vol. 7, no. 11, pp. 1583-1589, July 18 2013.

[4] L. Yi, "System modeling and identification of unmanned quad rotor air vehicle based on subspace and PEM," 2016 IEEE Systems and Technologies for Remote Sensing Applications Through Unmanned Aerial Systems (STRATUS), Rochester, NY, 2016, pp. 9-13.

[5] K. U. Lee, Y. H. Choi and J. B. Park, "Position control of a quadrotor: Dynamic surface control approach," The SICE Annual Conference 2013, Nagoya, Japan, 2013, pp. 1574-1579.

[6] R. Godwin, Ed., "Surveyor: Lunar Exploration Program, The NASA Mission Reports," Apogee Books Box 62034 Burlington, Ontario, Canada: Apogee Books, 2006.

[7] G. Scholz, M. Popp, J. Ruppelt and G. F. Trommer, "Model independent control of a quadrotor with tiltable rotors: IEEE/ION PLANS 2016, April 1114, Savannah, Georgia, United States of America," 2016 IEEE/ION Position, Location and Navigation Symposium (PLANS), Savannah, GA, 2016, pp. 747-756.

[8] D. Gheorghi, I. Vntu, L. Mirea and C. Brescu, "Quadcopter control system," 2015 19th International Conference on System Theory, Control and Computing (ICSTCC), Cheile Gradistei, 2015, pp. 421-426.

[9] G. Jithu and P. R. Jayasree, "Quadrotor modelling and control," 2016 International Conference on Electrical, Electronics, and Optimization Techniques (ICEEOT), Chennai, 2016, pp. 1167-1172.

[10] M. Ryll, H. H. Biilthoff, P. R. Giodano, "Modeling and control of a quadrotor uav with tilting propellers", Robotics and Automation (ICRA) 2012 IEEE International Conference on, pp. 4606-4613, May 2012.

[11] M. Ryll, H. H. Biilthoff, P. R. Giodano, "First flight tests for a quadrotor uav with tilting propellers", IEEE International Conference on Robotics and Automation 2013, 2013.

[12] F. enkul and E. Altu, "Modeling and control of a novel tilt Roll rotor quadrotor UAV," 2013 International Conference on Unmanned Aircraft Systems (ICUAS), Atlanta, GA, 2013, pp. 1071-1076.

[13] M. Elfeky, M. Elshafei, A. W. A. Saif and M. F. Al-Malki, "Quadrotor with tiltable rotors for manned applications," 2014 IEEE 11th International Multi-Conference on Systems, Signals & Devices (SSD14), Barcelona, 2014, pp. 1-5.

[14] A. F. enkul, . Y. Gelbal and E. Altu, "Manufacturing and flight tests of a quadrotor UAS with tiltable rotors," 2016 International Conference on Unmanned Aircraft Systems (ICUAS), Arlington, VA, 2016, pp. 752-757.

[15] A. Wojtulewicz, P. Chaber and M. awryczuk, "Multiple-input multiple-output laboratory stand for process control education," 2016 21st International Conference on Methods and Models in Automation and Robotics (MMAR), Miedzyzdroje, 2016, pp. 466-471.

[16] M. T. Ha and C. G. Kang, "A motion control system developed for research and education purposes," 2013 13th International Conference on Control, Automation and Systems (ICCAS 2013), Gwangju, 2013, pp. 46-49.

[17] I. Gaponov and A. Razinkova, "Quadcopter design and implementation as a multidisciplinary engineering course," Proceedings of IEEE International Conference on Teaching, Assessment, and Learning for Engineering (TALE) 2012, Hong Kong, 2012, pp. H2B-16-H2B-19.

[18] Aurora 9 - 9 Channel 2.4 GHz Aircraft Computer Radio, accessed on 7 July 2017, https://www.amazon.com/Aurora-2-4GHz-Transmitter-Optima-Receiver/dp/B002US3E4O

[19] Optima 9 - 9 Channel 2.4 GHz Receiver, accessed on 7 July 2017, http://hitecrcd.com/products/aircraft-radios-receivers-and-accessories/2.4ghz-aircraft-receivers-modules/optima-9-9-channel-2.4ghz-receiver/product

[20] PPM Encoder, accessed on 16 July 2017, http://ardupilot.org/copter/docs/common-ppm-encoder.html

[21] PX4 ardupilot, accessed on 7 July 2017, https://pixhawk.org/modules/pixhawk

[22] H. Ahmed and M. Tahir, "Accurate Attitude Estimation of a Moving Land Vehicle Using Low-Cost MEMS IMU Sensors," in IEEE Transactions on Intelligent Transportation Systems, vol. 18, no. 7, pp. 1723-1739, July 2017.

[23] S. Sabatelli, M. Galgani, L. Fanucci and A. Rocchi, "A Double-Stage Kalman Filter for Orientation Tracking With an Integrated Processor in 9-D IMU," in IEEE Transactions on Instrumentation and Measurement, vol. 62, no. 3, pp. 590-598, March 2013.

[24] Pixhawk Overview, accessed on 7 July 2017, http://ardupilot.org/copter/docs/common-pixhawk-overview.html

[25] AXI 4120/18 GOLD LINE — AXI Model Motors, accessed on 22 July 2017, https://www.modelmotors.cz/product/detail/238/

[26] W. Khan and M. Nahon, "Modeling dynamics of agile fixed-wing UAVs for real-time applications," 2016 International Conference on Unmanned Aircraft Systems (ICUAS), Arlington, VA, 2016, pp. 1303-1312.

[27] V. M. Arellano-Quintana, E. A. Portilla-Flores, E. A. Merchan-Cruz and P. A. Nio-Suarez, "Multirotor design optimization using a genetic algorithm," 2016 International Conference on Unmanned Aircraft Systems (ICUAS), Arlington, VA, 2016, pp. 1313-1318.

[28] HS-5685MH Metal Gear Digital Sport Servo, accessed on 22 July 2017, http://hitecrcd.com/products/servos/sport-servos/digital-sport-servos/hs-5685mh-high-torque-hv-metal-gear-servo-/product

[29] CSEPHXICE50 Castle Creations Phoenix Ice 50 33.6V ESC Remote Controlled Hobby, accessed on 22 July 2017, http://www.gravesrc.com/castle-creations-phoenix-ice-50-33-6v-esc.html

[30] ZIPPY Flightmax 3000mAh 5S1P 20C, accessed on 22 July 2017, https://hobbyking.com/en_us/zippy-flightmax-3000mah-5s1p-20c.html

[31] HobbyKing Quadcopter Power Distribution Board XT60 XT-60 20a Quad Mutlicopter 3.5mm, accessed on 22 July 2017, https://www.amazon.com/Quadcopter-Power-Distribution-Board-Mutlicopter/dp/B00QGCILK2

[32] CC BEC PRO Switching Regulator, accessed on 22 July 2017, http://www.castlecreations.com/en/cc-bec-pro-010-0004-01

[33] P. Castillo, R. Lozano and A. Dzul, "Stabilization of a mini-rotorcraft having four rotors," 2004 IEEE/RSJ International Conference on Intelligent Robots and Systems (IROS) (IEEE Cat. No.04CH37566), 2004, pp. 2693-2698 vol.3.

[34] Beard, Randal, "Quadrotor Dynamics and Control Rev 0.1" (2008). All Faculty Publications. 1325. Accessed on 23 July 2017, http://scholarsarchive.byu.edu/facpub/1325

[35] A. Dzaba and E. Schuster, "Nonlinear control of a dual-quadrotor assembly," 2013 American Control Conference, Washington, DC, 2013, pp. 223-228.

[36] A. Dzaba, E. Mucasey, A. Abraham, T. Hart and E. Schuster, "State-feedback control of the SpaceHawk Earth-based lunar hopper," 2013 International Conference on Unmanned Aircraft Systems (ICUAS), Atlanta, GA, 2013, pp. 628-633.

[37] Copter Attitude Control, accessed on 8 July 2017, http://ardupilot.org/dev/docs/apmcopter-programming-attitude-control-2.html

[38] J. V. C. Vilela, L. F. C. Figueredo, J. Y. Ishihara and G. A. Borges, "Quaternion-based H kinematic attitude control subjected to input time-varying delays," 2015 54th IEEE Conference on Decision and Control (CDC), Osaka, 2015, pp. 7066-7071.

[39] Yun Yu, Shuo Yang, Mingxi Wang, Cheng Li and Zexiang Li, "High performance full attitude control of a quadrotor on SO(3)," 2015 IEEE International Conference on Robotics and Automation (ICRA), Seattle, WA, 2015, pp. 1698-1703.

[40] K. Alexis, G. Nikolakopoulos and A. Tzes, "Model predictive quadrotor control: attitude, altitude and position experimental studies," in IET Control Theory and Applications, vol. 6, no. 12, pp. 1812-1827, Aug 16 2012.

[41] Robert McDowall. "Fundamentals of HVAC Control Systems," Elsevier Science, April 16 2009, IP Ed edition, pp. 21.

[42] Mandatory Hardware Configuration, accessed on 8 July 2017, http://ardupilot.org/copter/docs/configuring-hardware.html

Vita

Zhuogang Peng, son of Li and Mingxia Peng, was born in Songzi, Hubei, China on March 14, 1994. As an undergraduate, Zhuogang pursued a B.S. degree in Mechanical Engineering at Huazhong University of Science and Technology in Wuhan, China, and graduated in June of 2015. He then attended Lehigh University in Bethlehem, Pennsylvania, USA. Zhuogang is currently seeking a M.S. degree in Mechanical Engineering with an anticipated graduation date of August 2017.